Green Chemistry

Accepted Manuscript

ROYAL SOCIETY OF CHEMISTRY

www.rsc.org/greenchem

A Large-scale Synthesis of Heteroatom (N and S) co-doped Hierarchically Porous Carbon (HPC) Derived from Polyquaternium for Superior Oxygen Reduction Reactivity

Mingjie Wu[a], Jinli Qiao[a,d*], Kaixi Li[c], Xuejun Zhou[a], Yuyu Liu[b,e*], Jiujun Zhang[d,f]

Abstract: A simple, large-scale and green synthetic route is demonstrated for the preparation of polyquaternium derived heteroatom (N and S) co-doped hierarchically porous carbon (HPC). Our protocol allows for the simultaneous optimization of both porous structures and surface functionalities of (N and S) co-doped carbon (N-S-HPC). As a result, the obtained N-S-HPC shows a superior catalytic ORR performance to the commercial Pt/C catalyst in alkaline media, including high catalytic activity, remarkable long-term stability and strong methanol tolerance. Even in acidic media where most non-precious metal catalysts are suffered from high overpotential and low durability, our N-S-HPC exhibits an amazing ORR activity with a half-wave potential of 0.73V, and 40% enhanced limited diffusion-current density when compared to Pt/C catalyst. Particularly, when used for constructing a zinc–air battery cathode, such an N-S-HPC catalyst can give a discharge peak power density as high as 536 mW cm^{-2}. At 1.0 V of cell voltage, a current density of 317 mA cm^{-2} is achieved. This performance is superior to all reported non-precious metal catalysts in literature for zinc–air batteries and significantly outperforms the state-of-the-art platinum-based catalyst.

Keywords: Hierarchically porous carbons; nitrogen & sulfur co-doping; oxygen reduction reaction; fuel cells; metal-air batteries.

1

1. Introduction

The cathodic oxygen reduction reaction (ORR) is the sluggish and also the most challenging step in both polymer electrolyte membrane (PEM) fuel cells and metal–air batteries, which dominates the devices' performance[1,2] In the last several decades, extensive efforts have been made in speeding-up this reaction by exploring advanced electrocatalysts. Until now, the most practical ORR catalysts are still Pt-based materials, particularly for application in PEM fuel cells.[3,4] However, the drawbacks of the Pt-based catalysts, such as high cost, limited natural abundance and insufficient durability in harsh operation conditions are still not sufficiently addressed, hindering the large-scale commercialization of their associated technologies.[5] To overcome these challenges, great efforts have been made by exploring efficient, low-cost and durable non-precious metal catalysts to replace Pt-based ones.[6-10] Unfortunately, the majority of non-precious metal catalysts developed today are still suffered from insufficient catalytic ORR activity and low durability.[11-15]

It is known that the electrochemical reduction of oxygen is a multi-electron reaction

[a]*College of Environmental Science and Engineering, Donghua University, 2999 Ren'min North Road, Shanghai 201620, P. R. China, qiaojl@dhu.edu.cn*
[b]*Institute of Functional Materials, Donghua Universtiy, 2999 Ren'min North Road, Shanghai 201620, China*
[c]*Institute of Coal Chemistry, Chinese Academy of Sciences, Taiyuan, Shanxi 030001*
[e]*Multidisciplinary Research on the Circulation of Waste Resources,Graduate School of Environmental Studies, Tohoku University, Aramaki, aza Aoba 6-6-11, Aoba-ku, Sendai 980-8579, Japan, liu@mail.kankyo.tohoku.ac.jp*
[e]*Energy, Mining & Environment, National Research Council of Canada, Vancouver, BC, Canada, Jiujun.Zhang@nrc-cnrc.gc.ca*

that has two main possible pathways: one involving gain of $2e^-$ to produce H_2O_2, and the other, a direct $4e^-$ pathway to produce water. To obtain maximum energy capacity, it is highly desirable to reduce oxygen via the $4e^-$ pathway.[16] Oxygen reduction reaction (ORR) $2H_2O + O_2 + 4e^- \rightarrow 4HO^-$ in alkaline solution or $2H^+ + O_2 + 4e^- \rightarrow 2H_2O$ in acidic solution, significantly affects the electrochemical performance of fuel cells and metal-air batteries.[17] In the continuing effort to further improve the ORR performance of carbon-based catalysts, specific surface area, porous structure and surface functionalities have been identified as the targets for further optimization. It has been confirmed that introducing heteroatoms (e.g., B, P, S, N) into carbon materials to create ORR active sites has been seen to be much effective for performance enhancement.[18-20] Doping carbon with heteroatoms with electronegativity different from C (χ = 2.55) may create a net positive charge on adjacent carbon atoms. This effect makes such doped carbon material catalysts readily facilitate side-on O_2 surface adsorption, thus effectively weakening the O-O bonding[21] and leading to a high ORR catalytic activity. In this regard, nitrogen (χ = 3.04)-doped nanostructured porous carbon materials represent one kind of the important catalyst candidates, which are normally metal-free with high specific surface area and porous structure.[22-25] It has been identified that these catalysts' morphologies and the microstructures of their agglomerate play the most important roles in their ORR performance. Most recently, carbons co-doping with N and another element, for instance, B (χ = 2.04)[26] and P (χ = 2.16)[27] as well as O (χ = 3.44)[28] with higher electronegativity, have shown even higher ORR catalytic activity than the corresponding single-atom-doped counterparts. This co-doping with two elements that have different electronegativity is believed to create a unique electronic structure with a synergistic coupling effect between heteroatoms. With respect to this, N and S co-doped carbons, possessing a certain amount of mesoporous distribution, were synthesized and some exceptional ORR catalytic activity was also observed recently.[14,20,28]

However, in order to obtain the specified morphology and predetermined microstructure, the mesoporous carbon are usually synthesized using a sacrificial support method (SSM), during which the excess amount of hydrofluoric acid (HF) has to be added to remove the silica and also other metal-containing precursors commonly.[14,29,30] In addition, as some literature reported, the microporosity could be created by outside NH_3 activation.[3,31] Although some progresses have been achieved by carefully exploring suitable precursors and optimizing the nanostructuring process[32-36], the catalysts' ORR performances seem still inferior to the state-of-the-art Pt-based catalyst in terms of both catalytic activity and stability, particularly in strong acidic electrolytes, which is probably due to the non-ideal pore size distribution and low density of active sites.

Here we demonstrate a facial fabrication of heteroatom (N and S) co-doped hierarchically porous carbon (N-S-HPC) for oxygen reduction reaction by combining a simple silicate

templated two-step graphitization of the impregnated carbon derived from nitrogen-enriched polyquaternium-2 (PQ-2) without needing any outside NH_3 activation (The process is shown in **Fig. 1**). In particular, we use excess amounts of sodium hydroxide to re-

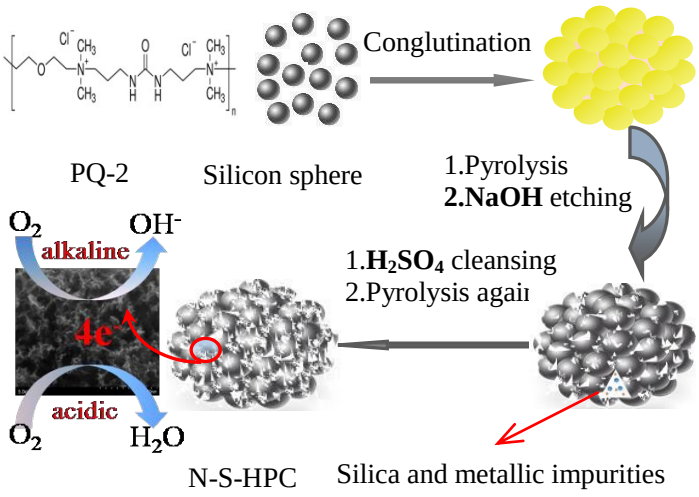

Fig. 1 A proposed mechanism for the synthesis process of N-S-HPC electrocatalyst.

move the silica instead of hydrofluoric acid. In this way, a large-scale production of such a catalyst can be easily realized and, it can also avoid environmental pollution caused by using hydrofluoric acid and ammonia. The N and S co-doped carbon catalyst shows a high specific surface area of 1,201 m^2 g^{-1}, and hierarchically porous structure composed of micro-, meso- and macro- pores. The synergistic effect is evidently observed, which should be induced by high density of catalytic ORR active sites and hierarchical pore structures facilitating excellent reactant transport. As a result, the catalysts have superior catalytic ORR performance to a Pt-based catalyst (Pt/C) in alkaline medium. Even in acidic media, where most non-precious metal catalysts are suffered from high overpotential and low durability, N-S-HPC exhibits an amazing ORR activity (half-wave potential of 0.73V) which is very close to the Pt/C catalyst under the same measuring conditions. In addition, the obtained N-S-HPC catalyst also presents the excellent long-term stability and high methanol tolerance. To demonstrate the potential of our catalyst for real energy devices, we have constructed a Zn–air battery using N-S-HPC catalyst as the air cathode, which gives a peak power density of 536 mW cm^{-2}. At 1.0 V of cell voltage, a current density of 317 mA cm^{-2} is achieved. The outstanding electrochemical performance of such a catalyst thereby makes it very promising for non-precious catalyst to replace the commercial Pt/C in both PEM fuel cells and metal-air batteries.

2.Results and discussion

2.1 Physical characterization

The morphology and microstructure of as-prepared N-S-HPC catalysts were investigated by means of scanning electron microscopy (SEM), transmission electron microscopy (TEM) and X-ray diffraction (XRD). It can be seen that N-S-HPC catalyst shows a sponge-like structure and, the disordered pores are cast successfully in the resultant carbon materials (SEM image in **Fig. S1(a)**). It is worthwhile to note that some interconnected macropores with diameters of 50-150 nm on the surface of the N-S-HPC sample can be observed, which do not directly replicate the sizes and shape of the used silica template (500 nm), suggesting that the macropores may collapsed during NaOH etching. TEM images, as shown in **Fig. 2(a),(b)** and **Fig. S1(b)**, reveal that the N-S-HPC is

consisted of a disordered pore system with the average diameter of 20 nm and a shell thickness of about 1nm, exactly reflecting the micro- and meso porous structure. From the XRD pattern (**Fig. S1(c)**), only two broad diffraction peaks (23º and 43º) can be explicitly observed, which correspond to the (002) and (004) planes of carbon materials with low graphitization, and indicate an entire amorphous structure. Obviously, this structure is consistent with the sponge-like structure shown in **Fig. S1(a)**. The N_2 adsorption–desorption plots of N-S-HPC, as shown in **Fig. 2(c)**, exhibit a type-IV isotherm with a steep increase of nitrogen absorption at a relatively high pressure, indicating the existence of mesopores. However, the rapid rise at low pressure region also indicates the presence of micropores, which is consistent well with the TEM observations. Using these plots, it can be calculated that N-S-HPC has a BET surface area as high as 1,201 m^2 g^{-1}. For comparison, N and S co-doped (N-S-PC) catalyst prepared without using a silica template was also characterized. The BET specific surface area for this N-S-PC sample was about 630 m^2 g^{-1}, which is much smaller than that of N-S-HPC, demonstrating that the introduction of silica during the fabrication

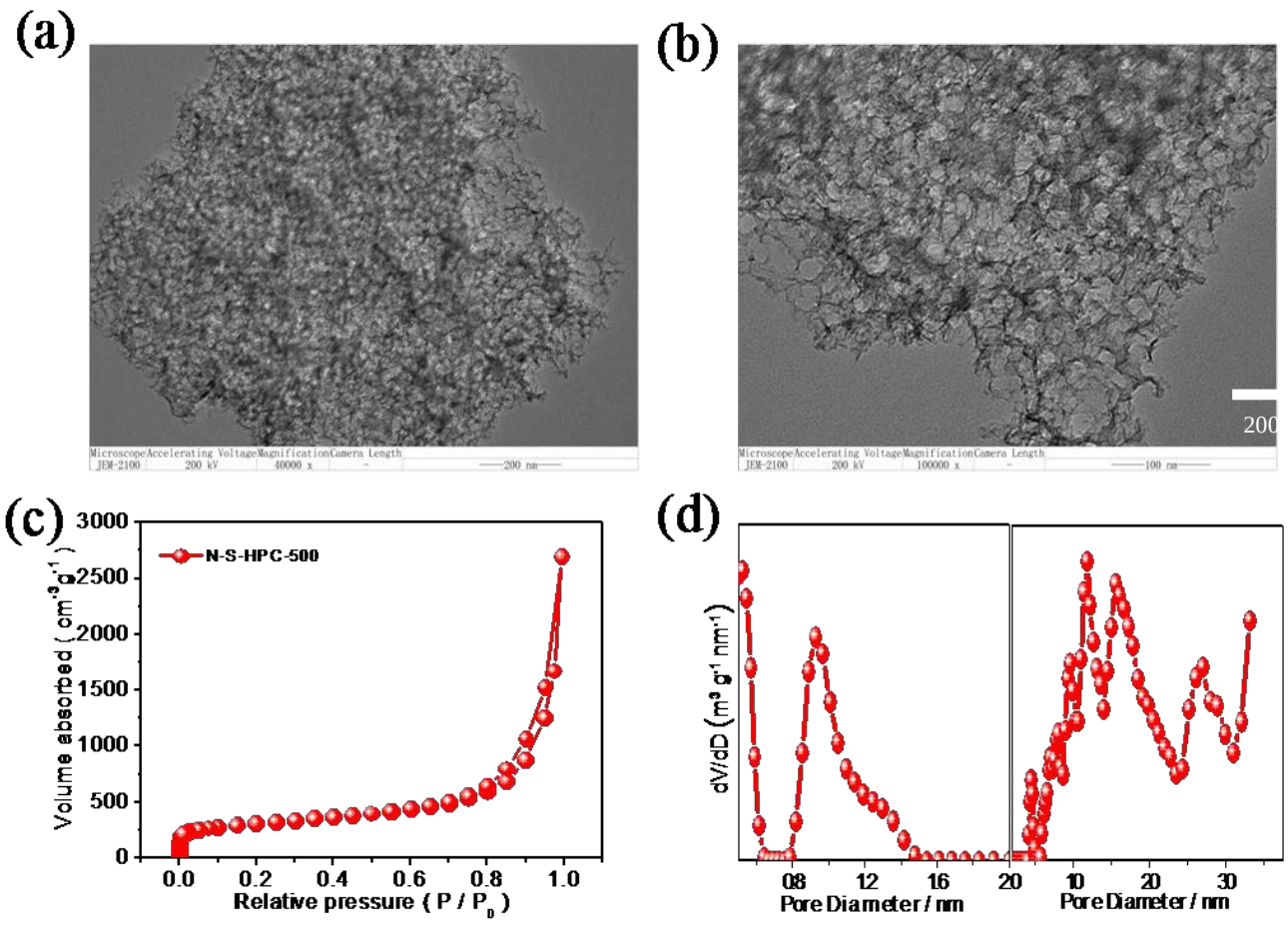

Fig. 2 TEM images of N-S-HPC catalyst with different magnifications, showing the highly porous structures. Scale bars: 200 (a) and 100 nm (b). (c) N_2 sorption isotherms of N-S-HPC; (d) Pore size distribution, determined using the BJH method.

process can effectively increase the surface area. This result is consistent with those reported elsewhere without using a silica template.[3,14]

The multimodal pore size distribution (PSD) plots **(Fig. 2(d)**) indicate that the N-S-HPC sample possesses micropores and mesopores centered at 1, 10, 15 and 28 nm, respectively, further confirming its hierarchical porous structure. As it is well-documented, the pore size distribution of the catalyst plays a key role in ORR activity, and hierarchical micro- and meso-porous structures can benefit the ORR activity due to the fact that active sites are predominately formed in the smaller micropores, while the larger pores can serve as reactive molecule reservoirs, and thus shorten the diffusion pathways of reactive molecules to and from the micropores. Hence, it is expected that N-S-HPC catalyst should be able to give a superior electrochemical performance for the ORR. It is believed that the high ORR performance could be promoted by large BET surface areas and appropriate pore structures.

Energy-dispersive X-ray spectroscopy (EDS) and X-ray photoelectron spectroscopy (XPS) were conducted to study the surface chemical composition of the samples. As shown in **Fig. 3 (a)** and **Fig. S1(d)**, in addition to C, N, O, S signals, there are no silica or metallic species detected for both of the N-S-HPC and N-HPC samples, suggesting that these Si and Fe species on the surface of N-S-HPC could be successfully removed by the leaching processes using NaOH solution and H_2SO_4. As

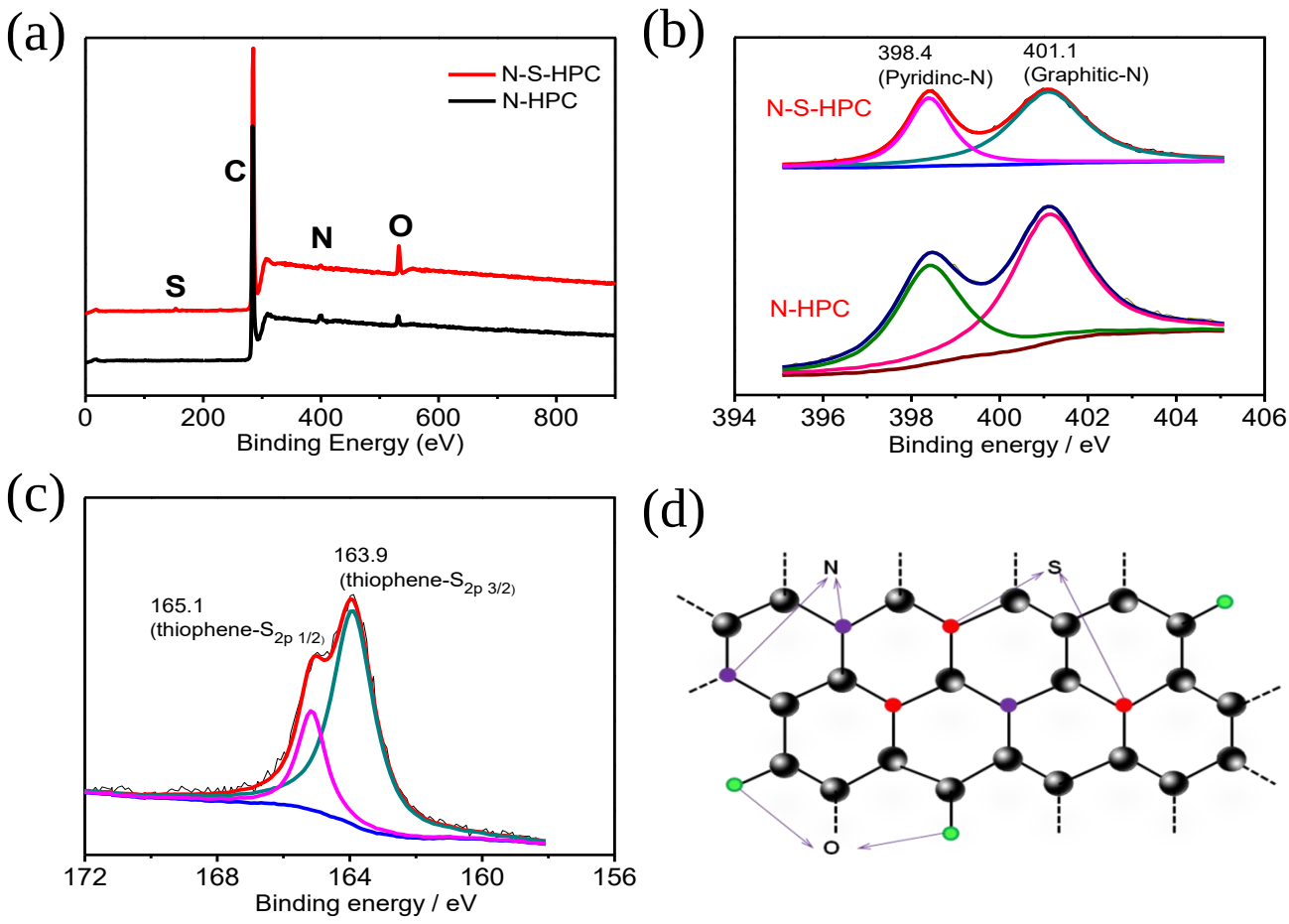

Fig. 3 (a) XPS spectra of N-S-HPC and N-HPC catalyst samples; (b) High-resolution N 1s XPS spectra of N-S-HPC and N-HPC; (c) High-resolution S 2p XPS spectra of N-S-HPC. (d) The postulated doping mechanisms in N-S-HPC.

demonstrated by both EDS and XPS analysis, N and S are both present in the N-S-HPC sample, demonstrating that N and S have been successfully doped into HPC by pyrolyzing the PQ-2 and ferrous sulfate mixture without addition of extra N or S sources, as illustrated in **Fig. 3(b) and (c)**. Additionally, FT-IR studies were also conducted proving that N and S were successfully incorporated into HPC. The absorption peaks at 1575 and 577 cm^{-1} are ascribed to the bending vibrations of C-N and C-S absorption, respectively **(Fig. S1(e))**. It has been known that doping carbon with heteroatoms may not only create more defects, but also lead to deformation of the carbon (open edge sites, high curvature), thus resulting in a sponge-like carbon structure.[14] Therefore, doping N and S may play these two beneficial roles, making contribution to the high BET surface area of the two samples partially. As discussed before, N-S-HPC has a high BET surface area of 1,201 m^2 g^{-1}, suggesting that the dual or multi heteroatom doping is indeed an effective way to improve BET surface area. According to the high resolution N 1s and S 2p spectra of the two samples (**Fig. 3(b) and (c)**), the calculated atomic percentages of different N, S and O functionalities are given in **Table 1**. Surprisingly, the final nitrogen content in N-S-HPC is only 3.9 at% when $FeSO_4$ $7H_2O$ is used as Fe source, while the content in N-HPC is 5.21 at.% when $FeCl_2$ $4H_2O$ as the Fe source. This may be explained by the fact that there is a competitive mechanism between nitrogen (N) and sulfur (S) as we reported previously [37]. As shown in **Fig. 3(b)**, the whole N1s spectra can generally be further divided into two primary peaks, corresponding to graphitic N (N1, 401.1 eV) and pyridinic N (N2, 398.4 eV), respectively[10], which are believed to play roles in the ORR process. Interestingly, the relative amount of graphitic N is increased from 59.2% for N-HPC to 78% for N and S co-doped N-S-HPC sample. Although the chemical process occurring during the sulfur introduction is not fully understood, these results clearly suggest that the synergistic effect induced by co-doping of N and S may not merely improve the porosity of N-S-HPC sample but also dramatically restructure its surface functionalities, both of which are crucial in enhancing the ORR activity. The binding energy of XPS-S_{2p} is also used to analyze the sulfur doping in S–N–HPC (**Fig. 3(c)**). As seen, the former two peaks are in agreement with the reported $S_{2p\ 3/2}$ (S1, 163.9 eV) and $S_{2p\ 1/2}$ (S2, 165.1 eV) positions of thiophene-S owing to their spin-orbit coupling,[38] while SO_x groups (168.5eV) are not evident. This suggests that SO_4^{-2} would be decomposed into S-containing small molecules (SO_X, H_2S, thiourea, etc.) during high temperature pyrolysis. According

Table 1. XPS Results of both N-S-HPC and N-HPC samples.

Catalysts	Total surface N content (at.%)	Surface content (at. %) of different N functionalities		Total surface S content (at.%)	Surface content (at. %) of different S functionalities		Total surface O content (at.%)
		N1	N2		S1	S2	
N-S-HPC	3.90	3.04	0.86	0.76	0.52	0.24	5.28
N-HPC	5.21	3.08	2.13				2.87

to Huang's report, carbon atoms at defect sites or oxygen-containing groups in carbon foams can react with thiourea to form C–S bonds.[38] We believe that the formation of C–S bonds in N-S-HPC may have a similar mechanism.These results further indicate that S and N atoms have been successfully doped into the carbon foams. **Fig. 3(d)** illustrates the postulated doping mechanisms in N-S-HPC.

2.2 Electrochemical measurements

Both the cyclic voltammetry (CV) and rotating disk electrode (RDE) measurements were performed to investigate the ORR activities of the developed catalysts. The N-S-HPC catalyst was tested in a N_2- and O_2-saturated 0.1 M KOH aqueous electrolyte solution using CV at a scan rate of 50 mV s^{-1} (**Fig. 4(a)**). In the case of a N_2-saturated solution, the cyclic voltammogram only presents a featureless quasi-rectangular trace with a typical characteristic of double layer

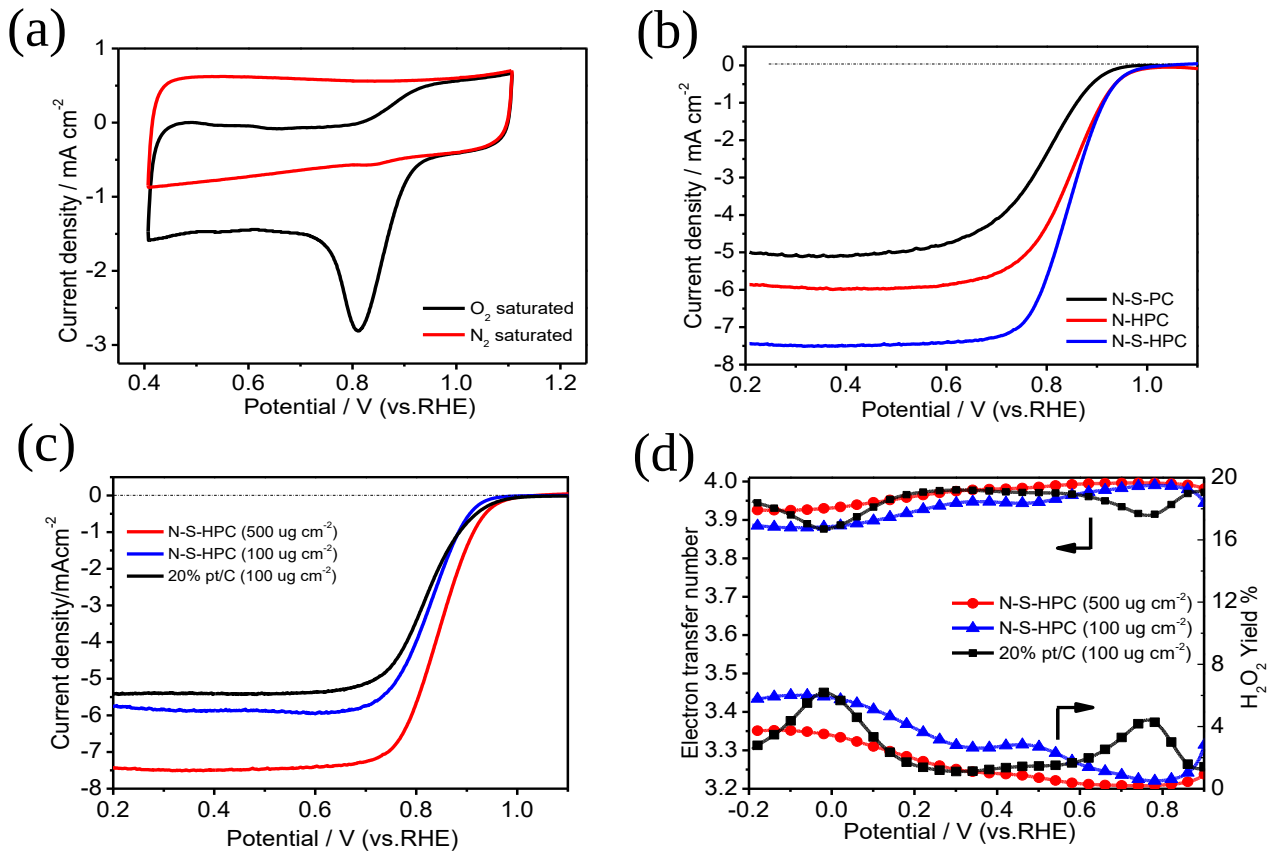

Fig. 4 (a) Cyclic voltammograms of a GC electrode coated by N-S-HPC catalyst (loading: 100 μg cm^{-2}), recorded in N_2- and O_2-saturated 0.1 M KOH at a scan rate of 50 mV s^{-1}; (b) Linear sweep voltammograms of various electrocatalysts on a rotating disk electrode (rotation rate: 1600 rpm) in O_2-saturated 0.1 M KOH at a scan rate of 5 mV s^{-1}; (c) Linear sweep voltammograms of N-S-HPC with 100 μg cm^{-2} and 500 μg cm^{-2} loadings, and Pt/C catalyst (20 wt% Pt, loading: 100 μg cm^{-2}), (d) Percentages of H_2O_2 produced and the electron transfer numbers of N-S-HPC catalysts and Pt/C catalyst.

capacitance of nitrogen-doped carbons. However, when O_2 was introduced into the solution, a distinct ORR response with the peak potential (E_p) at 0.813 V vs. RHE, and the peak current density (I_p) of 2.81 mA cm^{-2} can be clearly observed, indicating that this N-S-HPC catalyst has a profound catalytic ORR activity.

For a more quantitative analysis, **Fig. 4(b)** displays the typical ORR polarization curves for three catalyst samples (N-S-HPC, N-S-PC, and N-HPC) using RDE at a rotating rate of 1600 rpm for comparison. As can be seen from **Fig. 4(b)**, for N-S-HPC the values of onset potential (the onset potential was defined as the potential at which the background subtracted current density was equal to 0.1 mA cm^{-2}.[19]), half-wave potential ($E_{1/2}$) and catalytic current density (at 0.6 V) are 0.99V, 0.86V and 7.5 mA cm^{-2}, respectively, exhibiting a much enhanced electrocatalytic ORR activity when compared to both N-HPC and N-S-PC as well as previously reported results for heteroatom-doped carbon catalysts. Even with the low loading of 100 μg cm^{-2}, the N-S-HPC can still exhibit an excellent catalytic activity, as reflected by the $E_{1/2}$ of 0.83 V, which is more positive than the Pt/C catalyst ($E_{1/2}$ = 0.82 V) (**Fig. 4(c)**). This exceptional catalytic ORR activity of H-S-HPC catalyst may be induced by the relatively high BET surface area, proper pore structure, and high density of ORR-relevant active sites (including pyridinc-N, graphitic-N and thiophene-S). Considering the technical and economic feasibility, the catalyst loading of N-S-HPC was also increased to 500 μg cm^{-2} (**Fig. 4(c)**), yielding a significantly improved $E_{1/2}$ of 0.87 V, which is 40 mV more positive than that of Pt/C catalyst. Apart from the half-wave potential, the diffusion-limited current density of N-S-HPC approaches ~7.5 mA cm^{-2}, which is much higher than that of Pt/C (~5.5 mA cm^{-2}). To the best of our knowledge, these values including the half-wave potential and the diffusion-limited current density are superior to other non-precious metal catalysts reported to date, including metal-free ORR catalysts in an alkaline medium (**Table S1**). Obviously, the improved performance may be attributed to the synergistic effect, which includes the increased surface area, appropriate pore structures and high density of active sites.

In order to accurately quantify the ORR electron transfer pathway, rotating ring-disk electrode technique (RRDE)[12] was also employed in this work (**Fig. S2(a)**). The results revealed a high selectivity of the N-S-HPC catalyst towards the four-electron oxygen reduction. From **Fig. 4(d)**, it can be seen that the H_2O_2 yield measured with N-S-HPC catalyst (loading: 500 μg cm^{-2}) remains below 5% at all potentials and drops to 1.5% at 0.8 V, corresponding to a high electron-transfer number (n_e) of 3.97, which suggests a complete reduction of oxygen to water. This value is even slightly higher than that of Pt/C catalyst with a value of 3.92 at 0.8V. Even at a low loading of 100 μg cm^{-2}, the H_2O_2 yield is still remained below 6% at all potentials, demonstrating that N-S-HPC catalyst can indeed catalyze a complete 4-electron ORR.

Due to that the pyrolysis temperature can play an essential role in the formation of ORR active sites for non-precious metal catalysts, several temperatures such as 700, 800, and 900^{o}C were used to pyrolyze the N-S-HPC

samples for ORR catalysts. As shown in **Fig. S2(b)**, the most active catalyst is that synthesized at a pyrolysis temperature of 800^{o}C. In general, high temperatures can result in the decomposed species for active sites, while lower temperatures will not be sufficient to form densely populated active moieties.[1]

For direct methanol fuel cell application, catalyst's methanol tolerance is an important consideration. To test the methanol tolerance of the N-S-HPC catalyst, the chronoamperometric responses for both N-S-HPC and Pt/C catalysts were recorded in the presence of methanol in the electrolyte solution, as shown in **Fig. 5(a)**. It can be seen that after the addition of 3 M methanol to a 0.1 M KOH solution saturated with O_2, no noticeable change can be observed in the ORR current at the N-S-HPC electrode. However, the ORR current of Pt/C catalyst shows a drastic decrease once methanol is added under the same testing conditions. These results indicate that N-S-HPC catalyst has a super higher methanol tolerance than in the case for Pt/C catalyst.

The durability of both the N-S-HPC and Pt/C catalysts were also compared. We assessed the durability of the N-S-HPC catalyst using the US Department of Energy's accelerated durability test protocol. It can be seen that after 5000 continuous cycles the half-wave potential of N-S-HPC exhibited almost no any negative shift under O_2 cycling, which compares favorably with most non-precious metal catalysts and the Pt/C catalyst. Note, that a 35 mV of negative shift for Pt/C can be clearly observed after only 3000 continuous cycles (inset in **Fig. 5(b)**), indicating that N-S-HPC catalyst is very stable in alkaline solution.

Furthermore, the electrocatalytic performance of the catalysts obtained in acidic medium was also investigated. First, the CV curve indicates a significant reduction process for N-S-HPC, with a pronounced cathodic ORR peak at 0.625 V versus the reversible hydrogen electrode (RHE) when the electrolyte (0.5 M H_2SO_4) is saturated with O_2 **(Fig. S3(a)**). Normally, in acidic medium, most of non-precious metal catalysts are suffered from high overpotential and low durability. However, N-S-HPC exhibited a very promising ORR activity, as reflected by the $E_{1/2}$ of as high as 0.73 V, very close to the Pt/C catalyst ($E_{1/2}$ = 0.78 V) and, also much higher current density (～7.0 mA cm^{-2} at 0.50 V) than Pt/C catalyst (5.26 mA cm^{-2} at 0.50 V) (**Fig. 5(c)**). It can be found that for the electrode with a low catalyst loading (100 μg cm^{-2}), the ORR activity is very low and no well-defined limiting plateau can be observed (**Fig. S3(b)**). However, when the catalyst loading is increased to higher than 500 μg cm^{-2}, both onset potential and half-wave potential are greatly improved, and a comparatively well-defined mass-transfer-limited current plateau appears. It is noticed that the catalytic current densities (at 0.5 V) of the electrode with a loading of 800 μg cm^{-2} can reach 7.0 mA cm^{-2}, which is the highest value reported in the literature (**Table S2**). According to the RRDE polarization curves of N-S-HPC and commercial Pt/C at a rotation rate of 1600 rpm (**Fig. S3(c)**), the H_2O_2 yield calculated with N-S-HPC remains below 2.5% at all potentials and even much lower than Pt/C over the potential range of 0-0.5 V, showing an ORR process involving a complete 4-electron transfer pathway (n = 3.97-3.99) (**Fig. 5(d)**).

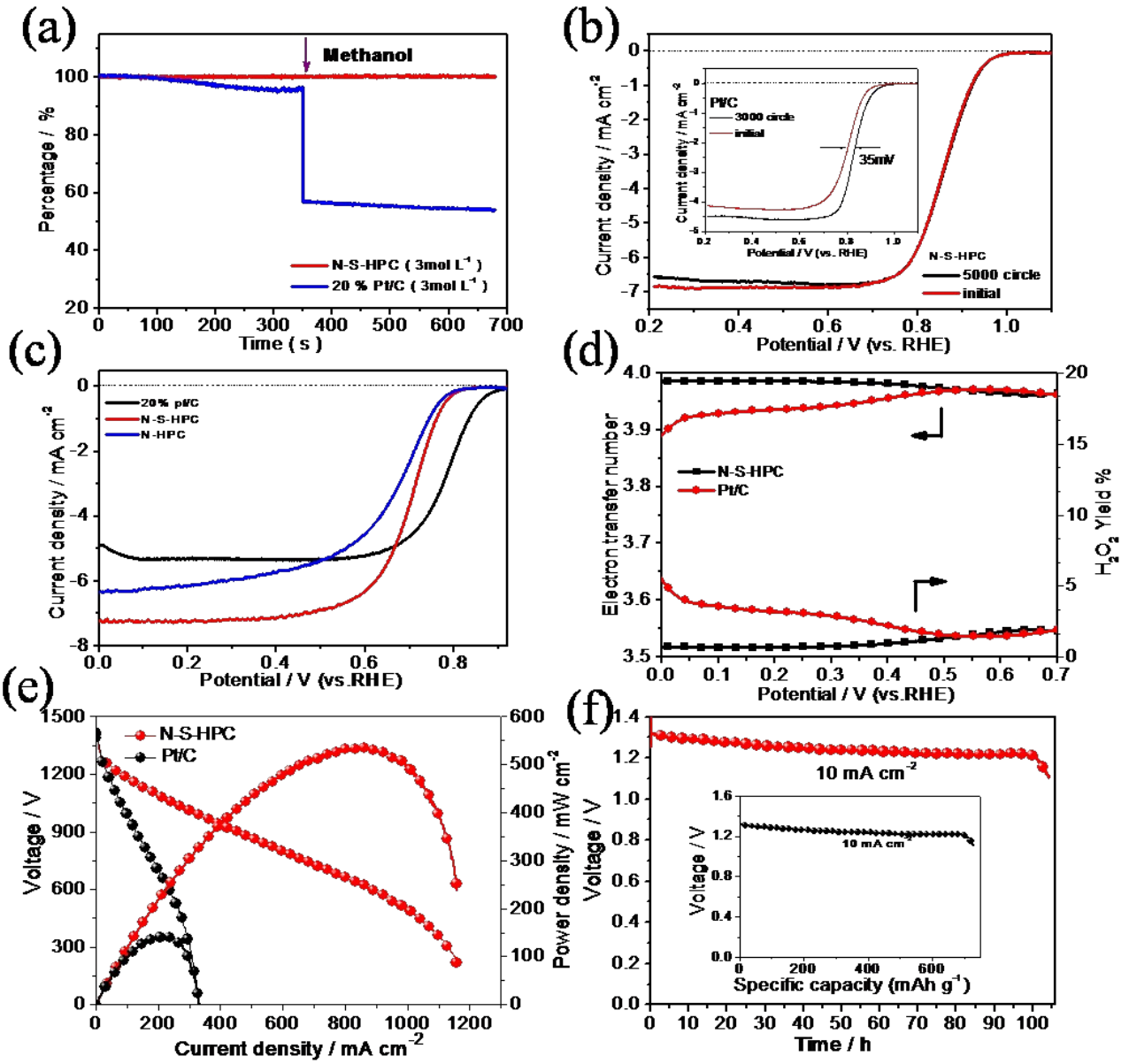

Fig. 5 (a) Chronoamperometric responses of N-S-HPC and Pt/C coated electrodes measured in O_2-saturated 0.1 M KOH with 3M methanol added; (b) Linear sweep voltammograms of N-S-HPC and Pt/C (inset) on a rotating disk electrode (1500 rpm) before and after 5000 cycles in O_2-saturated 0.1 M KOH at a scan rate of 5 mV s^{-1}; (c) Linear sweep ORR voltammetric curves for N-S-HPC, N-HPC and Pt/C. The loading was 0.8 mg cm^{-2} for all sample catalysts and 0.1 mg cm^{-2} for Pt/C. Electrolyte, 0.5 M H_2SO_4 for N-S-HPC-X and 0.1 M $HClO_4$ for Pt/C. Electrode rotation speed, 1600 rpm; scan rate, 5 mV s^{-1}; (d) Percentage of H_2O_2 produced and the electron transfer number of N-S-HPC catalysts (1600 rpm); (e) Single cell performance of the Zn–air battery showing polarization curve and power density with a comparison with Pt/C catalyst; (f) Long-time galvanostatic discharge curves of Zn–air cell with N-S-HPC as cathode catalyst at 10 mA cm^{-2} until complete consumption of Zn anode. The specific capacity was normalized to the mass of consumed Zn (inset). Electrolyte for Zn–air cell was 6.0 M KOH. Catalyst loading was 2.0 mg cm^{-2} for N/S-Fe-HPC.

Additionally, N-S-HPC exhibits a remarkable stability as well in acidic medium merely with a small negative shift of about 30 mV for the $E_{1/2}$ after 5000 continuous cycles under O_2 cycling (**Fig. S3(d)**).

To determine the role of iron in forming active ORR catalytic sites in the N-S-HPC, we investigated the ORR activity poisoning effect in both acidic and alkaline media containing 5 mM NaSCN (**Fig. S4**). Previous studies have revealed that introducing transition metals into the nitrogen containing complex could further enhance the ORR catalytic activity.[5] Transition metal, especially iron, was found to be indispensable to catalyze the graphitization of nitrogen−carbon precursor to form the highly graphitized carbon. However, the exact role of transition metals is still under debate whether the transition metal acts as the activity center or whether the transition metal only facilitates the formation of active nitrogen−carbon functional sites. In general, most electrochemical poisoning tests for studying the role of metals in the catalysts are conducted in alkaline media, and there are few electrochemical experiments performed in acidic medium, mainly due to the absence of appropriate ORR probes.[39] In our study , we employed SCN^- as a probe to further understand the role of iron in forming active sites in both acidic and alkaline media. Although no iron spectra could be found in the wide-scan spectra of the N/S-Fe-HPC, it does not mean that there is no metal residing in the catalyst due to the limited analytic sensitivity of XPS. In our work, inductively coupled plasma atomic emission spectrometry (ICP-AES) revealed an iron content of 0.3 wt%, confirming the presence of trace metals. According to the literatures most recently reported, even an extremely small amount of metallic impurities in carbon materials may have a strong influence on the ORR. As shown in **Fig. S4**, in the presence of SCN^- in 0.5 M H_2SO_4 electrolyte, the ORR onset potential of the N-S-HPC catalyst decreased significantly by more than 60 mV, with 1.35 mA cm^{-2} (19.3%) decrement in the diffusion-limiting current (**Fig. S4(a)**), suggesting blocking of the iron sites by SCN^- ions and a reduction of the electron transfer number from four-electron. After washing the catalyst to remove SCN^- ions absorbed on the active sites, the ORR activity is almost fully recovered, confirming that the Fe ion is the active center in the catalyst. Contrary to this completely, the N-S-HPC catalysts show almost no activity loss in the presence of SCN^- in 0.1 M KOH solution (**Fig. S4(b)**). These results likely suggest a very different catalytic mechanism and active site structures between acidic and alkaline media.[40]

To demonstrate the potential of our catalyst for practical energy devices, we constructed a Zn–air battery using N-S-HPC catalyst loaded on the gas diffusion layer (Tefloncoated carbon fibre paper) as the air cathode, Zn plate as the anode and 6M KOH as the electrolyte. As shown in **Fig. 5(e)**, the battery shows a very promising open circuit voltage of 1.415 V. At a voltage of 1.0 V, N-S-HPC reached a high current density of 317 mA cm^{-2}, which is much higher compared with the current density of 103 mA cm^{-2} obtained by 20%Pt/C at the same measuring conditions. In particular, the peak power density could be as high as 536 mW cm^{-2}, significantly superior to Pt/C (145 mW cm^{-2}) and also to those reported for Zn-air primary

batteries by applying N-doped CNTs (1V@ 50 mA cm^{-2}; 69.5 mW cm^{-2})[41] and N-doped porous carbon nanofibers (1V@ 150 mA cm^{-2}; 194 mW cm^{-2}).[42] Besides, the performance of our N-S-HPC based Zn–air battery in terms of both the current density at 1V and the peak power density is also significantly improved compared to those most recently reported Zn-air primary batteries by applying the metal oxides supported on carbon materials as cathode catalysts (**Table S3**). When the battery is galvanostatically discharged at 10 mA cm^{-2} for 100 hours, no obvious voltage drop can be observed until a complete consumption of the Zinc anode (**Fig. 5(f)**), again suggesting the durability of heteroatom (N and S) co-doped hierarchically porous carbon (N-S-HPC). The specific capacity normalized to the mass of consumed Zn was 730 mAh g^{-1} (inset graph in **Fig. 5 (f)**), corresponding to a high energy density > 900Wh kg^{-1} at discharge densities of 10 mA cm^{-2}.

Conclusions

In summary, heteroatom (N and S) co-doped hierarchically porous carbons (N-SHPC) using a simple and green two-step graphitization of the bis-quaternary ammonium group (PQ-2) have demonstrated an outstanding catalytic ORR performance. The unique hierarchical pore structures and high surface area can afford abundant active sites on the N-S-HPC surface and facilitate the electrolyte/reactant diffusion during the oxygen reduction process. The N-S-HPC catalyst doped with heteroatom (N and S) exhibits a surprisingly positive half-wave potential and high diffusion-limited current in both acidic and alkaline medium. Moreover, this catalyst shows both the pronounced electrocatalytic activity and long-term stability towards the ORR. The high-active and stable ORR performance can be attributed to the synergistic effects, which include the increased surface area, suitable pore structures and high density of active sites. The outstanding electrochemical performance of such catalysts thereby makes it very promising for this non-noble catalyst to replace the commercial Pt/C in both fuel cell systems and metal-air batteries.

3. Experimental section

3.1 Fabrication of polybasic controlled nanosilica template agents

With the purpose of obtaining the optimized hierarchical porous carbon materials, the first step in the synthesis was to prepare a template SiO_2 solution as follows: 5 g of nano-silica was mixed with 25 g of hydrochloric acid solution (1 M) and sonicated for eight minutes to easily obtain uniformly polybasic controlled nanosilica template agents (CNS) containing 16.6 wt.% of SiO_2.

3.2 Synthesis of nitrogen & sulfur-doped hierarchically porous carbons (N-S-HPC)

A hard-templating method combining a simple two-step graphitization of the impregnated carbon was used to synthesize the N & S-doped hierarchically porous carbon catalysts (N-S-HPC), as illustrated in **Fig. 1**. The N-S-HPC is synthesized by homogeneously dispersing iron and polyquaternium-2 (PQ-2) precursors onto the surface of SiO_2 template. In a typical synthesis process, 3.63g PQ-2 solution (62 wt.%, Sigma–

Aldrich,) was added into the pre-synthesized SiO_2 solution (the PQ-2 content as 45 wt.% with respect to the silica) under a magnetic stirring, resulting in the spontaneous coating of adherent PQ-2 layers. Then, a solution of $FeSO_4$ $7H_2O$ solution containing 0.3 g Fe was added into this mixture under stirring for more than 3 hours. Then the resulting viscous solution was dried for 48 hours at 85^{o}C. The obtained solid was ground to a fine powder in an agate mortar and, then pyrolyzed at 800^{o}C for 1 hour under a nitrogen atmosphere with a temperature ramp rate of 20^{o}C/min. The SiO_2 was leached out using excess amount of sodium hydroxide (NaOH) (4 M) solution for 48 hours. The resulting powder was washed by deionized water for neutralization, and then dried for overnight. To remove a redundant phase, mainly unreacted metallic iron and iron compounds, the sample was acid-leached using 0.5 M H_2SO_4 at 85^{o}C for 8 hours, then re-pyrolyzed at 800^{o}C for 1 hour under the same conditions as those during the first heat treatment to obtain the final catalyst sample. To confirm the synergetic effect between N and S, $FeCl_2$ $4H_2O$ was used as the Fe-precursor instead of $FeSO_4$ $7H_2O$ to prepare S-free counterparts, which is named N-HPC. Meanwhile, samples without using CNS (named N-S-PC) prepared by the same procedure were also used as the reference. For comparison, a state-of-the-art commercial Pt/C catalyst (20% Pt, BASF) was also measured under the same conditions.

Scanning electron microscopy (HITACHI/S-4800) was performed to observe the morphologies of various catalyst samples. To verify the microstructures of the samples, XRD patterns were collected by a Rigaku D/max-2550 V diffractometer with Cu Kα radiation operating at 30 kV and 40 mA. The specific surface area and pore size distribution curves were determined by nitrogen adsorption in a Micromeritics ASAP 2020 gas adsorption apparatus (USA). Surface analysis of the catalyst particles was carried out by XPS on a RBD upgraded PHI-5000C ECSA system (PerkinElmer) with Al K X-ray anode source (hn = 1486.6 eV) at 14.0 kV and 250 W.

Electrochemical measurements were performed in a conventional three-electrode cell using CHI Electrochemical Station (760D). All electrochemical tests were carried out in either O_2-saturated or N_2-saturated 0.1 M KOH electrolyte solution controlled at room temperature. In order to subtract the background capacitive current, linear sweep voltammetry was conducted under the same conditions in an N_2-saturated electrolyte. A platinum wire was used as the counter electrode and a saturated calomel electrode as the reference electrode, respectively. In this paper, all potentials were converted to the standard hydrogen electrode (SHE) scale. The catalyst ink was prepared by ultrasonically mixing 2.0 mg catalyst with 0.4 mL of isopropyl alcohol and 0.1 mL of 0.5 wt% Nafion® for more than 30 minutes. Then 6.0 µL (loading, 100 µg cm-2) or 31.0 μL (high loading, 500 μg cm^{-2}) of the resulting suspension was dropped onto the pre-cleaned GC (6.25 mm inner diameter and 7.92 mm outer diameter) surface, and dried at room temperature to form a uniform layer across the electrode surface. For comparison, a commercially available Pt/C catalyst (20 wt% Pt) was used as the baseline, and its electrode was prepared under the same conditions as those for the studied catalysts. Before each measurement for cyclic voltammograms (CV),

rotating-disk electrode voltammograms or chronoamperometry, the electrolyte solution was purged with high purity nitrogen or oxygen for at least 30 minutes to ensure saturation.

4. Supporting Information

Supporting Information is available from the Wiley Online Library or from the author.

5. Acknowledgements

This work was financially supported by the National Natural Science Foundation of China (21173039); The Project of Introducing Overseas Intelligence High Education of China (2015); the International Academic Cooperation and Exchange Program of Shanghai Science and Technology Committee (14520721900), and the College of Environmental Science and Engineering, State Environmental Protection Engineering Center for Pollution Treatment and Control in Textile Industry, Donghua University. All the financial supports are gratefully acknowledged.

[1] Y.J. Wang, D.P. Wilkinson and J. Zhang. Noncarbon Support Materials for Polymer Electrolyte Membrane Fuel Cell Electrocatalysts. *Chem. Rev*. 2011, 111, 7625.

[2] J.L. Qiao, L. Xu, L. Ding, L. Zhang, R. Baker, X.F. Dai, J.J, Zhang. Using pyridine as nitrogen-rich precursor to synthesize Co-N-S/C non-noble metal electrocatalysts for oxygen reduction reaction. *Appl. Catal., B: Environmental*. 2012, 125, 197.

[3] H.W. L, X.D. Zhuang, S. Bruller, X.L. F, K. Mullen. Hierarchically porous carbons with optimized nitrogen doping as highly active electrocatalysts for oxygen reduction. *Nat. Commun*. 2014, 5, 1.

[4] I. Morcos, E. Yeager. Kinetic studies of the oxygen-peroxide couple on pyrolytic graphite. *Electrochim. Acta*. 1970, 15, 953.

[5] G. Wu.，K.L. More，C.M. Johnston，Z. Piotr. High-performance electrocatalysts for oxygen reduction derived from polyaniline, iron, and cobalt. *Science*. 2011, 332, 443.

[6] D.Y. Qu. Investigation of oxygen reduction on activated carbon electrodes in alkaline solution. *Carbon*. 2007, 45, 1296.

[7] B.B. Blizanac, P.N. Ross, N.M. Markovic. Oxygen reduction on silver lowindex single-crystal surfaces in alkaline solution: rotating ring disk(Ag(hkl)) studies. *J. Phys. Chem*. 2006, 110, 4735.

[8] H.T. Chung, J.H. Won, P. Zelenay. Active and stable carbon nanotube/nanoparticle composite electrocatalyst for oxygen reduction. *Nat. Commun*. 2013, 4, 1922.

[9] J.C. Meier, I. Katsounaros, C. Galeano, H. J. Bongard, A.A. Topalov, A. Kostka, A. Karschin, F. Schuth, K.J.J. Mayrhofer. Stability investigations of electrocatalysts on the nanoscale. *Energ. Environ. Sci*. 2012, 5, 9319.

[10] Z.S. Wu, S. Yang, Y. Sun, K. Parvez, X.L. Feng, and K. Mullen. 3D nitrogen-doped graphene aerogel-supported Fe_3O_4 nanoparticles as efficient electrocatalysts for the oxygen reduction reaction. *J. Am. Chem. Soc*. 2012, 134, 9082.

[11] Y.G. Li, W. Zhou, H.L. Wang, L.M. Xie, Y.Y. Liang, F. Wei, J.C. Idrobo, S.J. Pennycook, H.J. Dai. An oxygen reduction electrocatalyst based on carbon nanotube-

graphene complexes. *Nat. Nanotechnol*. 2012, 7, 394.

[12] W. Xong, F. Du, Y. Liu, A. PerezJr, M. Supp, T.S. Ramakrishnan, L.M. Dai, Li Jiang. 3-D Carbon Nanotube Structures Used as High Performance Catalyst for Oxygen Reduction Reaction. *J. Am. Chem. Soc*. 2010, 132, 15839.

[13] C. Jin, T.C. Nagaiah, W. Xia, B. Spliethoff, S.S. Wang, M. Bron, W. Schuhmann, M. Muhler. Metal-free and electrocatalytically active nitrogen-doped carbon nanotubes synthesized by coating with polyaniline. *Nanoscale*. 2010, 2, 981.

[14] J.J. Shi , X.J. Zhou , P. Xu, J.L. Qiao, Z.W. Chen, Y.Y. Liu. Nitrogen and Sulfur Co-doped Mesoporous Carbon Materials as Highly Efficient Electrocatalysts for Oxygen Reduction Reaction. *Electrochim. Acta*. 2014, 145 , 259.

[15] A. Morozan,, B. Jousselme, S. Palacin. Low-platinum and platinum-free catalysts for the oxygen reduction reaction at fuel cell cathodes. *Energy Environ. Sci*. 2011, 4, 1238.

[16] D. Lei, X.F. Dai, L. Rui, H. Wang, J.L. Qiao. Electrochemical Performance of Carbon-Supported Co-Phthalocyanine Modified with Co-Added Metals (M = Fe, Co, Ni, V) for Oxygen Reduction Reaction. *J. Electrochem. Soc*. 2012, 159(9), 577.

[17] J.J. Shi, M.Y. Fan, J.L. Qiao, Y.Y. Liu. Nitrogen and chlorine dual-doped mesoporous carbon as efficient nonprecious electrocatalyst for oxygen reduction reaction both in alkaline and acidic electrolytes. *Chem. Lett*. 2014,43(9), 1484.

[18] Z. Liu, H. Nie, Z. Yang, J. Zhang, Z. Jin, Y. Lu, Z. Xiao, S. Huang. Sulfur-nitrogen co-doped three-dimensional carbon foams with hierarchical pore structures as efficient metal-free electrocatalysts for oxygen reduction reactions. *Nanoscale*. 2013, 5, 3283,.

[19] Z.P. Jin, H.G. Nie, Z. Yang, J. Zhang, Z. Liu, X.J. Xu and S.M. Huang. Metal-free selenium doped carbon nanotube/graphene networks as a synergistically improved cathode catalyst for oxygen reduction reaction. *Nanoscale*. 2012, 4, 6455.

[20] Z. Yang, Z. Yao, G.Y. Fang, G.F. Li, H.G. Nie, X.M. Zhou, X. Chen, S.M. Huang. Sulfur-doped graphene as an efficient metal-free cathode catalyst for oxygen reduction. *Acs Nano*. 2012, 6, 205.

[21] H. Wang, X. Bo, Y. Zhang, L. Guo, Sulfur-doped ordered mesoporous carbon with high electrocatalyticactivity for oxygen reduction. *Electrochim. Acta*. 2013, 108, 404.

[22] W. Yang, T.P. Fellinger, M. Antonietti. Efficient Metal-Free Oxygen Reduction in Alkaline Medium on High-Surface-Area Mesoporous Nitrogen-Doped Carbons Made from Ionic Liquids and Nucleobases. *J. Am. Chem. Soc*. 2011, 133, 206.

[23] D.S. Yu, Q. Zhang, L.M. Dai. Highly efficient metal-free growth of nitrogen-doped single-walled carbon nanotubes on plasma-etched substrates for oxygen reduction. *J. Am. Chem. Soc*. 2010, 132, 15127.

[24] C.V. Rao, C.R. Cabrera, Y. Ishikawa. In Search of the Active Site in Nitrogen-Doped Carbon Nanotube Electrodes for the Oxygen

Reduction Reaction. *J. Phys.Chem. Lett*. 2010, 1, 2622.

[25] S.Y. Wang, D.S. Yu, L.M. Dai, D.W. Chang, and J-B Baek. Polyelectrolyte-Functionalized Graphene as Metal-Free Electrocatalysts for Oxygen Reduction. *Acs Nano*. 2011, 5, 6202.

[26] S.Y Wang, E. Iyyamperumal, A. Roy, Y.H. Xue, D.S. Yu, L.M. Dai , Vertically Aligned BCN Nanotubes as Efficient Metal-Free Electrocatalysts for the Oxygen Reduction Reaction: A Synergetic Effect by Co-Doping with Boron and Nitrogen. *Angew. Chem*. 2011, 123, 11960.

[27] H.L. Jiang, Y.H Zhu, Q. Feng, Y.H. Su, X.L. Yang, and C.Z. Li, Nitrogen and Phosphorus Dual-Doped Hierarchical Porous Carbon Foams as Efficient Metal-Free Electrocatalysts for Oxygen Reduction Reactions. *Chem. Eur. J*. 2014, 20, 3106.

[28] R. Silva, D. Voiry, M. Chhowalla, T. Asefa, Efficient Metal-Free Electrocatalysts for Oxygen Reduction: Polyaniline-Derived N- and O-Doped Mesoporous Carbons. *J. Am. Chem. Soc*. 2013, 135, 7823.

[28] J. Liang, Y. Jiao, M. Jaroniec and S. Z. Qiao. Sulfur and Nitrogen Dual-Doped Mesoporous Graphene Electrocatalyst for Oxygen Reduction with Synergistically Enhanced Performance. *Angew. Chem. Int. Ed*. 2012, 51, 11496.

[29] A. Serov, M.H. Robson, K. Artyushkova. Highly active and durable templated non-PGM cathode catalysts derived from iron and aminoantipyrine. *Appl. Catal. B: Environ*. 2012, 127, 300.

[30] Y.L. Liu, C.X. Shi, X.Y. Xu, P.C. Sun, T.H. Chen. Nitrogen-doped hierarchically porous carbon spheres as efficient metal-free electrocatalysts for an oxygen reduction reaction. *J. of Power Sources*. 2015, 389.

[31] E. Proietti, F. Jaouen, M. Lefèvre, N. Larouche, J. Tian, J. Herranz,J.-P. Dodelet. Iron-based cathode catalyst with enhanced power density in polymer electrolyte membrane fuel cells. *Nat. Commun*. 2011, 2, 416 .

[32] K. Gong, F. Du, Z.H. Xia, M. Durstock, L.M. Dai. Nitrogen-doped carbon nanotube arrays with high electrocatalytic activity for oxygen reduction. *Science*. 2009, 323, 760.

[33] J. Zeng, C. Francia, C. Gerbaldi, M.A. Dumitrescu, S. Specchia, P. Spinelli. Substitute of Expensive Pt with Improved Electrocatalytic Performance and Higher Resistance to CO Poisoning for Methanol Oxidation: the Case of Synergistic Pt-Co_3O_4 Nanocomposite. *J. Solid State Electrochem*. 2012, 16, 3087.

[34] L. Zhang, J. Kim, E. Dy, S. Ban, K.C. Tsay, H. Kawai, Z. Shi, J. Zhang. Synthesis of novel mesoporous carbon spheres and their supported Fe-based electrocatalysts for PEM fuel cell oxygen reduction reaction. *Electrochim. Acta*. 2013, 108, 480.

[35] A. Serov, M.H. Robson, K. Artyushkova, P. Atanassov. Highly active and durable templated non-PGM cathode catalysts derived from iron and aminoantipyrine. J. Phys. *Applied Catalysis B: Environmental*. 2012, 127, 300.

[36] C.H. Choi, S.H. Park, S.I. Woo, Heteroatom doped carbons prepared by the pyrolysis of bio-derived amino acids as

highly active catalysts for oxygen electro-reduction reactions, *Green Chem*. 2011, 13 ,406.

[37] P. Xu, Q. Wang, T.S. Zhu, M.J. Wu, J.L. Qiao, W.Z. Chen, J.J. Zhang, Effects of transition metal precursors (Co, Fe, Cu, Mn, or Ni) on pyrolyzed carbon supported metalaminopyrine electrocatalysts for oxygen reduction reaction. *RSC Adv.* 2015, 5, 6195.

[38] Z. Liu, H.G. Nie, Z. Yang, J. Zhang, Z.P. Jin, Y.Q. Lu, Z.B. Xiao, S.M. Huang, Sulfur- nitrogen co-doped three-dimensional carbon foams with hierarchical pore structures as efficient metal-free electrocatalysts for oxygen reduction reactions. *Nanoscale*. 2013, 5, 3283.

[39] D. Singh, K. Mamtani, C.R. Bruening, J.T. Miller and U.S. Ozkan, Use of H_2S to Probe the Active Sites in FeNC Catalysts for the Oxygen Reduction Reaction (ORR) in Acidic Media. *Acs Catal*. 2014, 4, 3454.

[40] U. Tylus, Q. Jia, K. Strickland, N. Ramaswamy, A. Serov, P. Atanassov and S. Mukerjee, Elucidating Oxygen Reduction Active Sites in Pyrolyzed Metal–Nitrogen Coordinated Non-Precious-Metal Electrocatalyst Systems. *J. Phys. Chem. C*. 2014, 118, 8999.

[41] S.M. Zhu, Z. Chen, B. Li, D. Higgins, H.J. Wang, H. Li and Z.W. Nitrogen-doped carbon nanotubes as air cathode catalysts in zinc-air battery. Chen, *Electrochim. Acta*. 2011, 56, 5080

[42] G.S. Park, J.S. Lee, S.T. Kim, S. Park and J. Cho, Porous nitrogen doped carbon fiber with churros morphology derived from electrospun bicomponent polymer as highly efficient electrocatalyst for Zn–air batteries. *J. Power Sources*. 2013, 243, 267.